



Correlations between field capacity, porosity, solid particle density and dry density of a mechanically and biologically (biodried) treated reject waste stream

Igor Petrovic^{*}, Nikola Kaniski, Nikola Hrcic, Ivan Hip

Faculty of Geotechnical Engineering, University of Zagreb, Varazdin 42 000, Croatia

ARTICLE INFO

Keywords:

Solid particle density
Porosity
Bioreactor landfills
Field capacity
MBT

ABSTRACT

Several parameters are crucial for the proper functioning of bioreactor landfills (BL): field capacity (θ_k), porosity (n), solid particle density (ρ_s) and dry density (ρ_d). This paper considers the correlations between parameters, as measured on mechanically and biologically treated waste stream suitable for a BL. In total, 53 waste samples were tested and the n , ρ_s and ρ_d values were recorded. The related θ_k values were calculated from the modified ρ_d vs. θ_k relationship, published by Fungaroli and Steiner (1979). Through modified expressions, the following relationships were derived: second degree polynomial n vs. θ_k and first degree polynomial ρ_s vs. θ_k . In addition, the first degree polynomial ρ_d vs. n is proposed. The outlined relationships clearly highlight the contribution of n and ρ_s on corresponding θ_k values. Therefore, for optimal operating conditions of the BL, continuous monitoring of the mentioned parameters and proper adjustment of the θ_k value is necessary.

1. Introduction

Many landfill issues, such as containment, stability, settlement, gas generation, and leachate management, are common worldwide. Subsequent research efforts have focused more and more on providing a deeper scientific understanding of the complexities of the geotechnical behavior of mechanically and biologically treated (MBT) municipal solid waste (MSW) (Christensen et al., 1989; Cossu and Stegman, 2019; Zekkos, 2008).

The biological waste treatment process which has received significant attention over the last two decades is the biodrying process. The prime goals of the MBT plant, which utilizes the biodrying process, is the extraction of recyclable materials, production of refuse-derived fuel and separation of dry, organically rich reject waste stream, ready for depositing into a bioreactor (Velis et al., 2009). Once disposed of into bioreactor landfill, the reject fraction is subjected to an intensive wetting process to create a favorable environment for rapid microbial decomposition of the biodegradable solid waste (Reinhart and Townsend, 1998). Rapid biodegradation processes will increase the rate of methane production which can be extracted from the landfill body and, subsequently, used for energy recovery purposes. Therefore, bioreactor landfills are often seen as a viable waste-to-energy solution. However,

the design issues which must be considered, in order to secure the proper functioning of bioreactor landfills, require deeper understanding.

There are numerous environmental parameters which have a significant influence on the operational conditions of bioreactor landfill, namely: pH, temperature, nutrients, absence of toxins, moisture content, particle size and oxidation-reduction potential. One of the most critical parameters affecting MSW biodegradation has been found to be moisture content (Reinhart and Townsend, 1998). The target moisture content for optimal waste degradation is called field capacity (θ_k). By definition, θ_k is the residual volumetric moisture content after a prolonged period of gravity drainage (Reinhart and Townsend, 1998). Many researchers have published field capacity values obtained from different types of municipal solid waste (Beaven, 1999; Blight et al., 1992; Buivid et al., 1981; Gao et al., 2015; Stolz et al., 2012; Velásquez et al., 2003). A general conclusion that can be drawn from the published references is that the field capacity of waste material (expressed in volumetric terms) increases with an increase in the dry density (ρ_d). As the increase in density is dominated by volume reduction rather than a reduction in the volume of water, the increase in volumetric water content with dry density becomes apparent. However, only a few authors attempted to provide correlations between the dry density and field capacity of municipal solid waste, as summarized in Table 1.

^{*} Corresponding author.

E-mail addresses: igor.petrovic@gfv.unizg.hr (I. Petrovic), nikola.kaniski@gfv.unizg.hr (N. Kaniski), nikola.hrcic@gfv.unizg.hr (N. Hrcic), ivan.hip@gfv.unizg.hr (I. Hip).

<https://doi.org/10.1016/j.biteb.2022.100996>

Received 30 September 2021; Received in revised form 24 February 2022; Accepted 25 February 2022

Available online 28 February 2022

2589-014X/© 2022 Elsevier Ltd. All rights reserved.

Table 1
Dry density vs. field capacity correlations collected from the published literature.

Reference	Correlation
Fungaroli and Steiner (1979)	$\theta_k = 21.667 \ln(\rho_d) - 105.35$; where θ_k is field capacity [%] and ρ_d is dry density [kg/m^3]
Tchobanglous et al. (1993)	$\theta_{k,dry} = 0.6 - 0.55 \left(\frac{W}{44497.41 + W} \right)$; where $\theta_{k,dry}$ is the fraction of water in the waste, based on dry weight, and W is overburden weight calculated at the midheight of the waste in the lift in question [N]
Zornberg et al. (1999)	$\theta_k = 52.74 - 0.0771d$; where θ_k is volumetric field capacity [%] and d is depth below the waste surface [m] $\theta_f = \frac{\theta_i}{(1 - \Delta n)}$; where θ_f is final volumetric moisture content after compression [%]; θ_i is initial volumetric moisture content [%]; Δn is change in porosity
Lins et al. (2020)	$\theta_k = -0.083009\rho_d + 136.04$ -5 year old waste where θ_k is volumetric field capacity [%] and ρ_d is dry density [kg/m^3] $\theta_k = -0.02841\rho_d + 75.75$ -10 year old waste; where θ_k is volumetric field capacity [%] and ρ_d is dry density [kg/m^3]

Fungaroli (1971) found that field capacity significantly increases with a decrease in solid particle size while, with an increase in dry density, the increase of field capacity expressed in volumetric terms will asymptotically approach a particle size-dependent maximum. Interestingly, Lins et al. (2020) obtained a reversal trend among the mentioned parameters, as suggested by the negative gradient of the proposed correlation (Table 1).

As will be demonstrated later in the manuscript, the dry density is also a function of more fundamental properties, i.e. porosity (n) and solid particle density (ρ_s). Consequently, field capacity (θ_k) also depends on the porosity (n) and solid particle density (ρ_s) values. However, while the relationship between field capacity and dry density has been studied by several authors, its relationships with porosity (n) and solid particle density (ρ_s) remain mostly uninvestigated.

In bioreactor landfill, immediately after the wetting process is initiated, significant settlements occur, caused by increased moisture content. Since these settlements usually develop very quickly, a rapid decrease of porosity (n) under a constant $\rho_{s, const}$ value can be anticipated. With the progression of time, the settlements caused by the wetting process will cease and the decomposition processes begin. Subsequently, in the later operational stages of the bioreactor landfill, the decrease of ρ_s caused by the degradation process under a constant porosity (n_{const}) can be anticipated.

Therefore, it seems rational to clearly distinguish the contribution of porosity (n) and solid particle density (ρ_s) parameters to the field capacity value (θ_k). Thus, the research focus of the present paper was placed on the measurement of n , ρ_s and ρ_d values of biodried MBT reject waste material with particle size $D_{50} \approx 5.0$ mm and its relationship with corresponding θ_k values.

2. Materials and methods

2.1. Waste sample origin

Within the scope of the presented paper, all tests were conducted on mechanically and biologically (biodried) treated (MBT) reject waste stream, prepared for landfilling into a bioreactor landfill cell. The required waste samples were obtained immediately after the treatment process was finished and prior to the samples being sent to the landfill. The samples were taken from the MBT plant at Marišćina, an integral part of the Marišćina waste management center (WMC), located in Istria, Croatia. In order to encompass seasonal variations, samples from summer and winter seasons were collected.

2.2. MBT/MSW constituent composition

The constituent composition was determined for representative summer and winter samples, obtained by the quartering method. In total, four samples were examined (two from winter and two from summer). The individual waste components were manually separated into the following categories: plastics, textiles, glass, metals, paper/cardboard, wood, bones/skin, stones, ceramics, rubber and kitchen waste. Any unidentifiable particles were placed into the miscellaneous category, which was divided into two fractions: coarser particles (larger than 2 mm) and finer particles (less than 2 mm).

2.3. Moisture content, organic content, and maximum dry density of tested waste

In practice, the waste used for the testing described in the presented manuscript was landfilled into a bioreactor cell. In order to determine the initial conditions of the waste, once it had been landfilled, the moisture content, organic matter and maximum dry density of sampled waste material was established. The moisture content was determined in accordance with the ASTM D2216-19 standard (ASTM International, 2019). In order to reduce the risk of the mass loss of organic content, the drying temperature was set to 60 °C. The organic content was determined in accordance with the ASTM D2974-20e1 standard (ASTM International, 2020). The maximum dry density ($\rho_{d, max}$) to which the tested waste material can be compacted into the landfill body in its dry state, was determined according to the ASTM D4253 standard (ASTM International, 2016b). The $\rho_{d, max}$ value was established as an average value, obtained from seven independent measurements conducted on winter samples only.

2.4. Particle size analysis procedure

Particle size analysis was conducted on multiple waste samples from the winter and summer periods, in accordance with ASTM D422-63 standard (ASTM International, 2007). The averaged particle size distribution curve for waste from the winter period was obtained on 25 subsequently-tested samples, with the average mass of each individual sample being close to 1 kg. The averaged particle size distribution curve for waste from the summer period was obtained from 14 subsequently-tested samples, following an identical procedure to the winter samples.

2.5. Air pycnometer device

Measurement of the n and ρ_s parameters was conducted with a custom-made, constant-volume air pycnometer. A constant-volume air pycnometer consists of two chambers of known volume which are connected by an air pipeline and coupling valve. For the pressure chamber, an advanced pressure/volume controller (ADVDPCC) was used. For the sample chamber, two toxic interface units (<https://www.gdsinstruments.com/gds-products/toxic-interface-unit>) were used, interchangeably. A photograph of the setup used is presented in Fig. 1. The basic operating principle of a constant-volume air pycnometer is as follows: the sample chamber is kept under atmospheric pressure (relief valve open); the air in the pressure chamber is pressurized while the coupling valve is kept closed; the initial air pressure (p_1) within the pressure chamber is recorded; after the initial pressure (p_1) is recorded, the relief valve of the sample chamber is closed; the coupling valve is opened, in order to allow the pressurized air to expand into the sample chamber; when air pressure reaches a new equilibrium state, the air pressure (p_2) is recorded; based on the ideal gas law and measured air pressures (p_1) and (p_2), the volume of solid particles V_s and solid particle density ρ_s can be obtained. Further details about various techniques for measuring porosity (n) and free air space (FAS) can be found in Ruggieri et al. (2009).

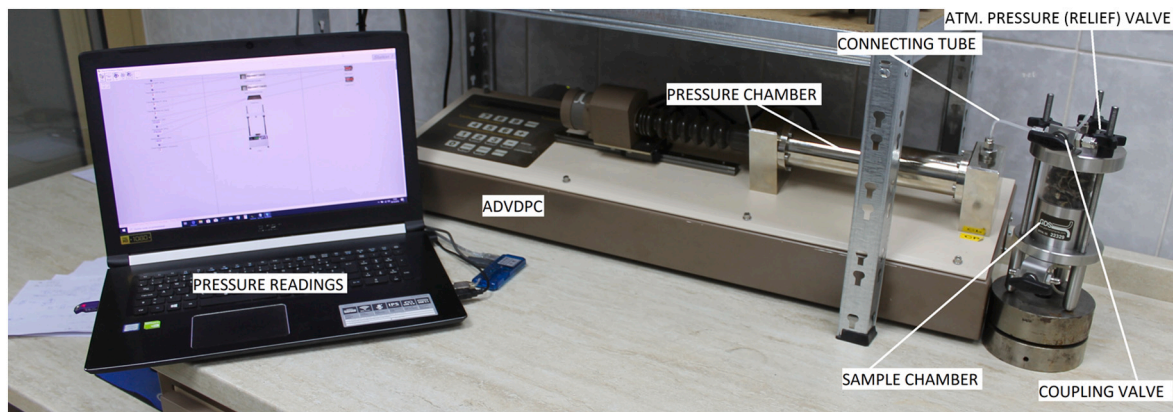


Fig. 1. Air pycnometer set-up used.

2.6. Testing procedure

For 33 winter and 20 summer waste samples, corresponding (n, ρ_s) pairs of values were measured with the air-pycnometer set-up described. The sample volume of all tested samples was $221.9 \times 10^{-6} \text{ m}^3 \pm 1.4 \times 10^{-6} \text{ m}^3$.

The mass of winter samples varied randomly and they were divided into two groups. The first group consisted of 23 samples, while the remaining 10 samples were placed into the second group. The larger group of samples was tested in an uncompacted state. The dry densities of winter samples in the uncompacted state varied randomly from 94 to 222 kg/m^3 . Before measurement of corresponding (n, ρ_s) values, the second group of samples were submitted to the compaction process on a vibrating table, in accordance with ASTM D4253-16e1 (ASTM International, 2016b) – test method 1A.

The summer samples were also separated into two groups, with 10 samples in each group. The sample mass in each group was kept constant at 0.026 and 0.082 kg, respectively. Thus, the dry densities of summer samples were kept constant at 118 and 370 kg/m^3 , respectively. The samples were tested in an uncompacted state.

3. Theory

3.1. Theoretical relationships between n , ρ_s and θ_k parameters

Porosity (n) is defined as the ratio between the volume of voids V_v and total volume V . The difference between porosity (n) and the volumetric moisture content is called free air space (FAS). Free air space is the void space which is freely available to microorganisms. In the dry state of the material, free air space (FAS) equals porosity (n). In the literature, FAS is mostly correlated with bulk density (ρ), solid particle density (ρ_s) and moisture content (w). The theoretical relationship between these parameters was proposed by Agnew et al. (2003) and is shown in Eq. (1).

$$FAS [\%] = 100 - \rho \left[\frac{w}{\rho_w} + \frac{100 - w}{\rho_s} \right] \quad (1)$$

where ρ is the bulk density, ρ_s is the solid particle density and ρ_w is the density of water (1000 kg/m^3).

A more comprehensive list of theoretical relationships between porosity, free air space and other relevant parameters can be found in Ruggieri et al. (2009).

For dry samples ($w = 0$; $\rho = \rho_d$) Eq. (1) reduces into Eq. (2), which then represents porosity (n):

$$n [\%] = 100 - \rho_d \left[\frac{100}{\rho_s} \right] \quad (2)$$

Rearranging Eq. (2) provides Eq. (3):

$$\rho_d = \frac{\rho_s (100 - n)}{100} \quad (3)$$

As opposed to soils, where solid particle density (ρ_s) can be considered constant, due to its strong heterogeneous nature and the decomposition process, the solid particle density (ρ_s) of waste materials is not a constant value. Therefore, the dry density (ρ_d) of waste materials expressed by Eq. (3) is a function of two variables: solid particle density (ρ_s) and porosity (n).

Solid particle density (ρ_s) is the ratio between the mass of solid particles m_s and the volume of solid particles V_s . The most comprehensive research into the ρ_s of waste materials was conducted by Yesiller et al. (2014). The authors investigated the influence of particle size, compaction, and degree of decomposition (aged waste) on ρ_s . They found that ρ_s increases with reduced particle size, compaction and degree of decomposition (aged waste). The authors attributed the increase of ρ_s to reduced particle size, compaction and the potential access of previously occluded intraparticle voids. For aged waste, the increasing ρ_s was attributed to the loss of biodegradable components with low ρ_s values. A similar influence of decomposition processes on the increase of waste solid particle density was observed by Reddy et al. (2011). Agnew et al. (2003) studied the influence of moisture content on ρ_s value, for a variety of organic materials (manure compost, MSW compost, biosolids, straw, woodchips, and leaves). The obtained results showed that increased moisture content decreases ρ_s due to an increased volume of solid particles caused by swelling. Conversely, increased moisture content can also weaken particle structure, causing the particles to collapse and, consequently, reducing the solid particle volume. Therefore, the ρ_s of waste material depends on its decomposition stage (organic content), the size of individual particles and moisture content. A more comprehensive set of ρ_s data gathered from the literature, which clearly indicates strong variability of ρ_s , is presented in Table 2.

Fungaroli and Steiner (1979) published several relationships between the dry density (ρ_d) and field capacity (θ_k) of milled refuse. In their research, five waste samples with different granulometric properties were tested. Eq. (4) presents the relationship between ρ_d and θ_k for fully saturated milled waste with particle size D_{50} equal to 4.8 mm.

$$\theta_k [\%] = 18.877 \ln(\rho_d) - 59.642 \quad (4)$$

With the insertion of Eq. (3) into Eq. (4), the theoretical relationship between the n , ρ_s and θ_k parameters for waste materials, with particle size D_{50} equal or close to 4.8 mm, can be obtained (Eq. (5)).

$$\theta_k [\%] = 18.877 \ln \left(\frac{\rho_s (100 - n)}{100} \right) - 59.642 \quad (5)$$

Eq. (5) shows that θ_k is not only correlated with ρ_d but it is also a function of the corresponding (n, ρ_s) pairs of values. A three-dimensional

Table 2
Solid particle densities (ρ_s) of various waste materials collected from the literature.

Ref.	ρ_s (kg/m ³)	Measurement method Water pycnometry (WP)/Air pycnometry (AP)	Additional information
Untreated waste			
Gabr and Valero, 1995	2000	WP	15 to 30-year-old waste. Test performed in accordance with the ASTM D854-83 standard (ASTM International, 2016a) on the entire grain-size distribution; five samples with a variance of 0.0032
	2400	WP	Test performed in accordance with the ASTM D854-83 standard on only the fine fraction (<No. 200 mesh); five samples with a variance of 0.0355
Zhu et al., 2003	1960–2620	–	Waste materials with grain size larger than 0.5 cm were removed
Olivier and Gourc, 2007	1030	Mercury bath	Average solid particle density of individual waste constituents
Reddy et al., 2009	850 ± 130 970 ± 60	WP WP	Fresh MSW, ASTM D854 Landfilled MSW, ASTM D854, waste subjected to low amounts of leachate recirculation, 1.5 years old
Stoltz et al., 2010	1650	AP	Average solid density value. Fresh MSW from French landfill, average value with standard deviation of 0.05
Breitmeyer, 2011	1340 ± 20	WP	ASTM D854; dry, shredded MSW
Hyun Il et al., 2011	2440–2540	–	Old, degraded
Yesiller et al., 2014	1072/1258	WP	Uncompacted/compacted; fresh
	2201	WP	1.5 years old; water pycnometry method samples taken from Santa Maria Regional Landfill located in California, USA.
Pulat and Yukselen-Aksoy, 2017	1120	WP	Fresh sample, Manisa landfill
	1430	WP	Degraded sample, Manisa landfill
Ramaiah and Ramana, 2017	1900–2150	WP	Ghazipur dumpsite, Delhi, ASTM D854-14
	1950–2550	WP	Okhla dumpsite, Delhi, ASTM D854-14
Thakur et al., 2019	1830–1920	WP	Dumpsite Una district of Himachal Pradesh, fresh
	1850–2280	WP	Dumpsite Una district of Himachal Pradesh, degraded
Mokhtari et al., 2019	1800	WP	Fresh sample, ASTM D854-10, Kahrizak landfill, Tehran
	2310	WP	5.5 year old waste, ASTM D854-10, Kahrizak landfill, Tehran
	2560	WP	14 year old waste, ASTM D854-10, Kahrizak landfill, Tehran

Table 2 (continued)

Ref.	ρ_s (kg/m ³)	Measurement method Water pycnometry (WP)/Air pycnometry (AP)	Additional information
	2610	WP	21 year old waste, ASTM D854-10, Kahrizak landfill, Tehran
Treated waste			
Agnew et al., 2003	1881 ± 34	AP	Moisture content 42%
	1725 ± 26	AP	Moisture content 55%
Hudson et al., 2004	876–1303	–	The waste was processed using the DANO technique prior to testing. Evolution of solid particle density with the vertical load. The vertical stress range went from 34 to 463 kPa
Entenmann and Wendt, 2007	1580–1980	Capillary pycnometer	Various waste mixtures
Rose et al., 2009	1902	WP	MSW compost, test method NBR 06508/1984 (ABNT(b), 1984)
Sudarshana, 2011	1690	Gas jar method	0–10 mm fraction size, average value
	1929	Gas jar method	0–20 mm fraction size, average value
Velkushanova, 2011	1630	Gas jar method	BS1377-2 (British Standards Institution, 1990)
Sivakumar Babu et al., 2015	1260	Density bottle method and pycnometer method	Mechanically and biologically treated compost reject collected from the Mavallipura landfill site
Synthetic waste			
Reddy et al., 2011	1090	WP	Fresh
	2050	WP	Anaerobic acid phase
	2260	WP	Accelerated methane phase
	2300	WP	Decelerated methane phase
	2470	WP	Methane stabilization
Yesiller et al., 2014	1377/1530	WP	Uncompacted/compacted
Pulat and Yukselen-Aksoy, 2017	1620	WP	European average MSW composition
	1240	WP	Turkish average MSW composition
	1840	WP	United States average MSW
Ke et al., 2017	1380	WP	Fresh sample
	2190	Water displacement method	Sample after 18 months of degradation

graphical representation of Eq. (5), obtained for theoretical pairs of (n , ρ_s) values, is presented in Fig. 2.

Fig. 2 reveals that θ_k increases with a decrease in n value caused by settlement processes and an increase in ρ_s value caused by degradation processes. In addition, Fig. 2 also reveals the existence of a non-linear correlation of n vs. θ_k and a linear correlation of ρ_s vs. θ_k . By projecting the 3D curve from Fig. 2 onto two-dimensional n - θ_k space, the n vs. θ_k relationship under a constant $\rho_{s,const}$ value can be obtained. In addition, by projecting the 3D curve from Fig. 2 onto two-dimensional ρ_s - θ_k space, the ρ_s vs. θ_k relationship under a constant n_{const} value can be obtained.

The non-linear n vs. θ_k relationship can be well-approximated with the second-degree polynomial (Eq. (6)).

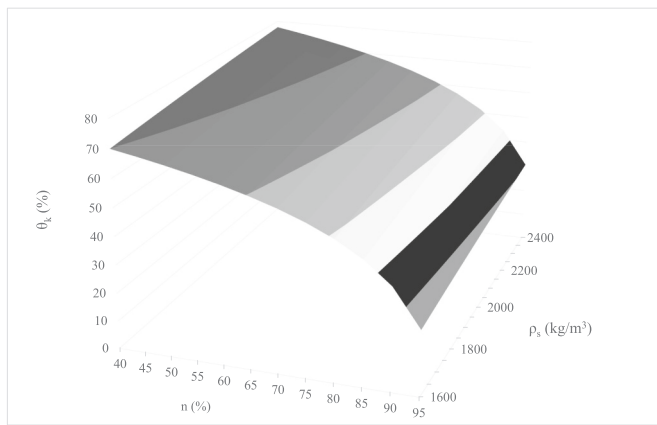


Fig. 2. Theoretical relationship between θ_k , n and ρ_s parameters.

$$\theta_k [\%] = -0.0154 \cdot n^2 + 1.3352 \cdot n + C_1 \quad (6)$$

The linear ρ_s vs. θ_k relationship can be expressed with a first degree polynomial (Eq. (7)).

$$\theta_k [\%] = 0.0095 \cdot \rho_s + C_2 \quad (7)$$

C_1 and C_2 are constants which are dependent on the selected $\rho_{s, const}$ or n_{const} value and can be estimated with Eqs. (8) and (9).

$$C_1 = 0.0098 \cdot \rho_{s, const} + 23.47 \quad (8)$$

$$C_2 = -0.0069 \cdot n_{const}^2 + 0.3154 \cdot n_{const} + 53.273 \quad (9)$$

Sensitivity analysis of Eq. (6) indicates that, for an increase of n value from 40% to 90%, over 50% decrease of θ_k can be expected. Similar analysis of Eq. (7) revealed that, for an increase of ρ_s value from 1600 to 2400 kg/m^3 , an increase of θ_k close to 10% can be expected. Clearly, θ_k is more sensitive to the variations of n values caused by settlement and compaction process than to the variations of ρ_s values caused by the degradation processes.

4. Results and discussion

4.1. Established constituent composition

Table 3 presents the obtained mean mass percentages of individual constituents of the winter and summer samples. Table 3 reveals that more than 60% of waste material could not be identified as a result of intensive treatment processes. From the identifiable portion of the material, three main components (with the highest mass percentages) can be distinguished: plastics, paper/cardboard, and glass. With respect to

Table 3
Constituent composition of tested waste material.

Component	Mass [%]	
	Winter period	Summer period
Plastics	6.43	5.27
Textiles	0.22	0.53
Glass	10.62	8.95
Metals	0.94	0.97
Paper/cardboard	4.71	5.45
Wood	1.18	5.27
Bones/skin	0.20	0.35
Stones	2.76	5.01
Ceramics	0.46	0.75
Rubber	0.13	0.40
Kitchen waste	2.15	2.83
Miscellaneous >2 mm	42.48	35.52
Miscellaneous <2 mm	27.71	28.70
Total	100	100

the influence of waste composition on field capacity values, Gao et al. (2015) found that waste materials with high kitchen waste content generally have higher field capacity values than the waste materials with low kitchen waste content. Based on their findings, the constituent composition of the tested waste material (Table 3) might suggest that the field capacity of the tested material is relatively low, due to the fact that kitchen waste is only present in small percentages. However, since more than 60% of tested samples remained unidentified, this observation is not conclusive.

4.2. Emplacement conditions

The established moisture and organic content of winter samples were 9.60% and 51.6%, respectively. For summer samples, the determined moisture and organic content were 10.13% and 55.26%, respectively. The established average maximum dry density ($\rho_{d, max}$) of tested waste material was 383 kg/m^3 . The determined moisture content percentages reveal that tested waste material is landfilled in a rather dry state and, consequently, with very low microbiological activity. The established percentage of organic content reveals that the tested material possessed a high potential for methane production and energy recovery purposes. According to the information obtained from the Marišćina landfill manager, once landfilled, the tested material achieves an emplacement density close to 380 kg/m^3 .

In summary, the tested material is deposited into the landfill body at densities which are close to the maximum achievable values under dry conditions and at a moisture content which is significantly below its field capacity value.

4.3. Particle size distribution curves

Fig. 3 presents averaged granulometric curves obtained from tested samples. The results indicate similar granulometric properties among the samples from different seasons, although the summer samples have a smaller amount of coarser (>31.5 mm) particles and a larger amount of finer (<4 mm) particles. The difference between the particle size distribution curves from summer and winter specimens can be explained by the tourist season during the summer period, which has a significant influence on waste composition and particle size distribution. In addition, Fig. 3 presents a particle size distribution curve of the milled waste sample tested by Fungaroli and Steiner (1979). Clearly, the waste material tested by Fungaroli and Steiner (1979) and the waste samples tested within this research share similar granulometric properties. Based on the similarity of granulometric properties among the samples used within this research and the granulometric properties of samples obtained by Fungaroli and Steiner (1979) the validity of Eq. (5) for tested waste material can be assumed.

4.4. Measured pairs of (n ; ρ_s) values

The measured pairs of (n ; ρ_s) values of summer and winter samples are presented in Table 4. As can be seen from Table 4, V_v values obtained on summer samples lie in the range from 206.5×10^{-6} to $210.49 \times 10^{-6} \text{ m}^3$ with a mean value of $208.56 \times 10^{-6} \text{ m}^3$ and standard deviation of $\pm 1.46 \times 10^{-6} \text{ m}^3$. V_v values obtained on winter samples lie in the range from 194.85×10^{-6} to $212.62 \times 10^{-6} \text{ m}^3$ with a mean value of $202.73 \times 10^{-6} \text{ m}^3$ and standard deviation of $\pm 3.81 \times 10^{-6} \text{ m}^3$. Clearly, the obtained results reveal that tested material is highly porous with large void spaces.

It is interesting to note that (n ; ρ_s) pairs of values obtained on both groups of summer samples differed from each other, although the ρ_d of each group was kept constant. The variation of (n ; ρ_s) values under constant ρ_d can be attributed to the heterogeneous nature of waste material. Moreover, a more thorough investigation of the results obtained from summer samples (Table 4) reveals the existence of a linear relationship between n and ρ_s under a constant ρ_d value.

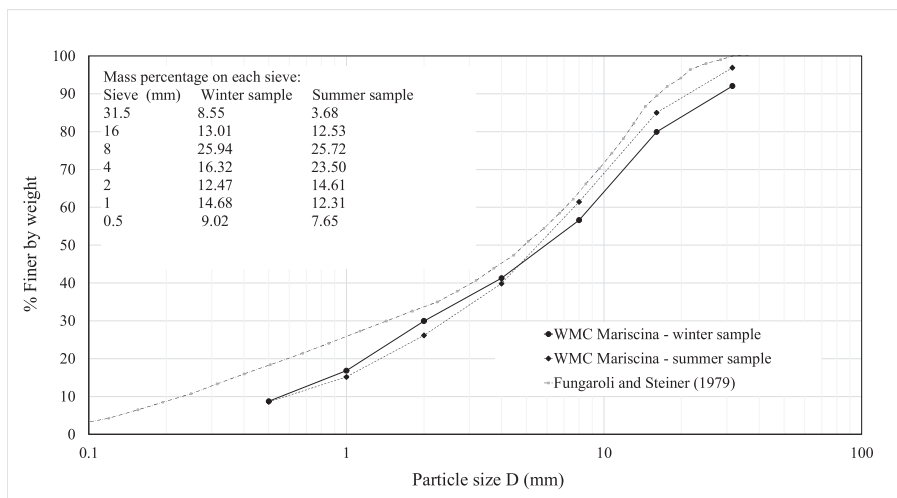


Fig. 3. Particle size distribution curves of tested waste material.

For comparison purposes, Table 4 also presents pairs of (n ; ρ_s) values and corresponding field capacity values, collected from the literature by Gao et al. (Gao et al., 2015). From the collected data, several observations can be made. With the exclusion of the results obtained by Wei (2007), who observed the opposite trend, data published by other researchers clearly reveals the existence of a general trend of increasing field capacity values with a decrease of n value. In addition, the results obtained by Wu et al. (2012) revealed that an increase of solid particle density causes an increase of field capacity. Interestingly, even though the n and solid particle density values varied significantly among the tested waste materials, the dry density in the presented cases lie within a much narrower range of values. This is most obvious when comparing the results published by Wu et al. (2012) and Breitmeyer and Benson (2011). While both authors tested waste material with fairly similar dry densities, the obtained field capacity values significantly differ. These findings clearly indicate that field capacity is not only a function of the dry density, but it also depends on the more fundamental properties like n , ρ_s and particle size.

In addition, it is also interesting to note that the insertion of appropriate values of dry density and solid particle density (presented in Table 4) into Eq. (2) provides reliable predictions of n values, comparable with measured n values (Table 4).

4.5. n vs. θ_k and ρ_s vs. θ_k correlations

Based on the measured dry density (ρ_d) and related pairs of (n ; ρ_s) values, the corresponding θ_k values can be obtained using either Eq. (4) or Eq. (5). While both equations provide the same result, the main advantage of Eq. (5) is its ability to clearly differentiate the individual contribution of n and ρ_s parameters to the corresponding field capacity value.

In Figs. 4 and 5, 23 pairs of (ρ_d ; θ_k) values are represented with white squares. While the ρ_d of each point is measured, the corresponding field capacity value is calculated using Eq. (4). The presented results indicate that, in Eq. (4), an increase of ρ_d will be followed by a corresponding increase of field capacity. In addition, Fig. 4 presents two-dimensional n - θ_k space with 23 pairs of (n ; θ_k) values at corresponding ρ_s values obtained on winter samples. ρ_s and n values of each sample were measured and the appropriate field capacity value was calculated with Eq. (5). Fig. 4 clearly shows that the same θ_k value can be obtained for various combinations of (n ; ρ_s) values.

Moreover, Fig. 4 reveals that the presented pairs of (n ; θ_k) are conveniently grouped around a narrow range of corresponding ρ_s values. In Fig. 4, each group is denoted by a different marker shape. Based on Eqs. (6) and (8), the corresponding curves for the $\rho_{s,const}$ values,

determined as an average value of each group individually, are also presented. For example, nine (n ; θ_k) values with corresponding ρ_s values lie in a narrow range from 1812 kg/m³ to 1900 kg/m³ and are closely grouped around the theoretical curve obtained with the $\rho_{s,const}$ value set to 1857.2 kg/m³. The presented example clearly demonstrates how the settlements caused by the wetting process in the early operational stage of the bioreactor landfill, can influence the field capacity value under the assumption that solid particle density remains unchanged.

Similarly, Fig. 5 presents two-dimensional ρ_s - θ_k space with 23 pairs of (ρ_s ; θ_k) values at corresponding n values obtained from winter samples and it reveals that presented pairs of (ρ_s ; θ_k) values formed several groups around narrower ranges of corresponding n values. In Fig. 5, each group is represented by different marker shapes. Based on Eqs. (7) and (9), the corresponding curves at n_{const} values, determined as an average value of each group individually, are also presented. For example, five (ρ_s ; θ_k) pairs with corresponding n values lie in a narrow range from 89.17 to 89.79% and are closely grouped around the averaged curve, attained at the n_{const} value set to 89.64%. This case clearly demonstrates the influence of the degradation processes on the increase in the field capacity value in the later operational stages of the bioreactor landfill, under the assumption that any further decrease of porosity is negligible.

4.6. ρ and ρ_d vs. n correlations

4.6.1. Uncompacted samples

Based on the raw data presented in Agnew and Leonard (2002), the ρ_d vs. n relationship for MSW compost by linear regression is derived (Eq. 10). The obtained relationship shows that ρ_d and n are inversely proportional parameters.

$$n_{MSW,compost} [\%] = -0.075\rho_d + 106.03 \quad (10)$$

Fig. 6 presents 23 (ρ_d ; n) data records obtained on winter samples. For comparison purposes, Fig. 6 presents the ρ_d vs. n relationship for tested winter samples and the n values calculated using Eq. (10). Comparison shows that the negative slope value obtained on tested material is significantly lower than the negative slope value in Eq. (10). Clearly, with respect to the tested material, the MSW compost tested by Agnew and Leonard (Agnew and Leonard, 2002) was less stiff material and the smaller particle sizes were prone to produce a greater decrease of n value for the same amount of increase in dry density. In addition, Fig. 6 confirms the inverse proportionality of the ρ_d and n parameters.

Based on the data records, the ρ_d vs. n relationship of tested waste material can be expressed by Eq. (11).

$$n [\%] = -0.0495\rho_d + 99.354 \quad (11)$$

Table 4

Obtained n and ρ_s values.

Sample no./reference	$V_v \times 10^{-6}$ [m ³]	n [%]	Calculated field capacity value – Eqs. (4) or (5) [%]	Calculated n value – Eq. (2) [%]	Dry density [kg/m ³]	ρ_s [kg/m ³]
Summer samples						
1	206.50	93.35	30.34	93.35	118	1767
2	207.15	93.64	30.34	93.64	118	1849
3	207.20	93.67	30.34	93.67	118	1856
4	207.49	93.80	30.34	93.80	118	1895
5	208.48	94.25	30.34	94.25	118	2043
6	208.48	94.25	30.34	94.25	118	2043
7	209.48	94.70	30.34	94.70	118	2217
8	209.81	94.85	30.33	94.85	118	2281
9	210.49	95.15	30.34	95.15	118	2425
10	210.49	95.15	30.33	95.15	118	2425
Average	208.56	94.28	30.34	94.28	118	2080
St. dev.	±1.46	±0.66	±0.00	±0.66	±0	±244
1	171.97	77.93	52.00	77.94	370	1677
2	175.73	79.63	52.00	79.64	370	1817
3	175.72	79.63	52.00	79.64	370	1817
4	176.83	80.13	52.00	80.14	370	1863
5	176.96	80.19	52.00	80.20	370	1869
6	177.68	80.51	52.00	80.53	370	1900
7	177.94	80.63	52.00	80.64	370	1911
8	179.43	81.31	52.00	81.31	370	1980
9	179.67	81.41	52.00	81.42	370	1992
10	182.04	82.49	52.00	82.50	370	2114
Average	177.40	80.38	52.00	80.40	370	1894
St. dev.	±2.58	±1.17	±0	±1.17	±0	±112
Winter samples						
1	194.85	88.08	42.34	88.08	222	1863
2	200.51	90.64	37.26	90.64	170	1812
3	202.77	91.66	36.70	91.66	165	1974
4	198.62	89.79	39.03	89.79	186	1824
5	199.89	90.36	39.66	90.36	193	1998
6	206.88	92.41	34.03	92.41	143	1882
7	205.18	91.65	34.61	91.65	147	1765
8	199.90	89.29	40.47	89.29	201	1877
9	201.99	90.22	39.61	90.22	192	1964
10	203.00	90.67	37.28	90.67	170	1820
11	201.99	90.22	37.28	90.22	170	1736
12	207.09	92.50	34.04	92.50	143	1906
13	201.99	90.22	38.71	90.22	183	1873
14	206.05	92.04	37.76	92.04	174	2187
15	206.05	92.04	37.27	92.04	170	2131
16	202.59	90.49	36.26	90.49	161	1691
17	204.93	91.53	36.26	91.54	161	1900
18	199.63	89.17	41.29	89.17	210	1938
19	200.27	89.46	38.24	89.45	179	1694
20	198.67	88.74	40.47	88.74	201	1785
21	206.51	92.24	33.44	92.24	138	1785
22	212.62	94.97	26.08	94.97	94	1865
23	200.69	89.64	41.29	89.64	210	2027
Average	202.73	90.78	37.36	90.78	173	1882
St. dev.	±3.81	±1.54	±3.48	±1.54	±29	±123

From the published references

	n [%]	Measured field capacity [%]	–	Dry density [kg/m ³]	ρ_s [kg/m ³]
Zhan et al. (2008)	72.6	32.4	–	410	–
	68.4	36.5	–	610	–
	64.0	41.3	–	720	–
Wu et al. (2012)	65.5	31.5	–	520	1510
	62.1	34.8	–	710	1880
	55.6	36.9	–	950	2140
Wei (2007)	66.6	36.6	–	–	–
	66.6	36.7	–	–	–
	75.0	39.2	–	–	–

Table 4 (continued)

From the published references					
	n [%]	Measured field capacity [%]	–	Dry density [kg/m ³]	ρ_s [kg/m ³]
	75.0	41.1	–	–	–
	80.0	46.0	–	–	–
Breitmeyer and Benson (2011)	60.0	24.1	–	561	1320–1360
	53.1	27.9	–	632	
	40.8	20.3	–	795	

Dissimilar gradients in Eqs. (10) and (11) also suggest that different kinds of treatment processes, i.e., composting vs. biodrying, produce final products with different physical properties. Therefore, regardless of whether both wastes are colloquially called ‘MBT waste’, the equations which correlate the physical properties of one material should not be interchangeably used on other types of waste material.

With respect to the summer samples, Fig. 6 presents n values of summer samples at dry densities of 118 and 370 kg/m³, respectively. Strong variation of n under constant dry density values, because of waste heterogeneity, is obvious. Extrapolation of Eq. (11), obtained for winter samples, to a dry density value equal to 370 kg/m³, reveals that Eq. (11) is capable of accurately predicting the n value of summer samples as well. It seems that the proposed Eq. (11) is rather insensitive to the seasonal variations in waste constituents, as long as the treatment process produces materials with similar granulometric properties.

Additionally, Agnew et al. (2003) also proposed ρ vs. FAS relationships that were valid for MSW compost material (Eq. (12)) and a more general relationship (Eq. (13)), which is applicable to the various waste materials.

$$FAS_{MSW,compost} [\%] = -0.0894\rho + 102.69 \tag{12}$$

$$FAS [\%] = -0.09\rho + 100 \tag{13}$$

where ρ is the wet bulk density (kg/m³) and FAS is free air space. Eqs. (11) and (12) reveal that ρ and FAS are also inversely proportional parameters.

For illustration purposes, Fig. 6 also presents FAS values calculated with Eq. (12), under the assumption that volumetric moisture content (VMC) in all winter samples increases from zero to 40%. Based on this assumption, appropriate bulk densities were established and inserted into Eq. (12). Clearly, the free air space (FAS) available to microorganisms will also be significantly reduced due to filling of the voids with water, caused by the wetting process. Even though similar behavior can be anticipated for the material tested in this study, in order to obtain the appropriate relationship, further research under wet conditions is necessary.

4.6.2. Compacted samples

The influence of compaction on the ρ_s parameter and ρ_d vs. n relationship was also examined. The obtained ρ_s values on compacted samples were in the range from 1655 to 2041 kg/m³, with an average value equal of 1914 kg/m³ and standard deviation of ±115.25 kg/m³. The obtained results reveal that compaction only has a moderate influence on the increase of ρ_s for the tested material. The mean ρ_s value obtained on compacted samples only increased by 1.7%, with respect to the mean ρ_s value obtained on uncompacted samples (Table 4). The obtained results suggest that compaction during emplacement of the tested waste material into the landfill body should not have a detrimental effect on ρ_s and, ultimately, it should not have a major influence on the initial θ_k value.

The increase in ρ_s was most likely caused by the removal of closed pores within the larger, more porous, particles. Increase in ρ_s due to compaction was also confirmed by Yesiller et al. (2014). However, in their research, the increase in ρ_s was significantly higher (16.6%), most

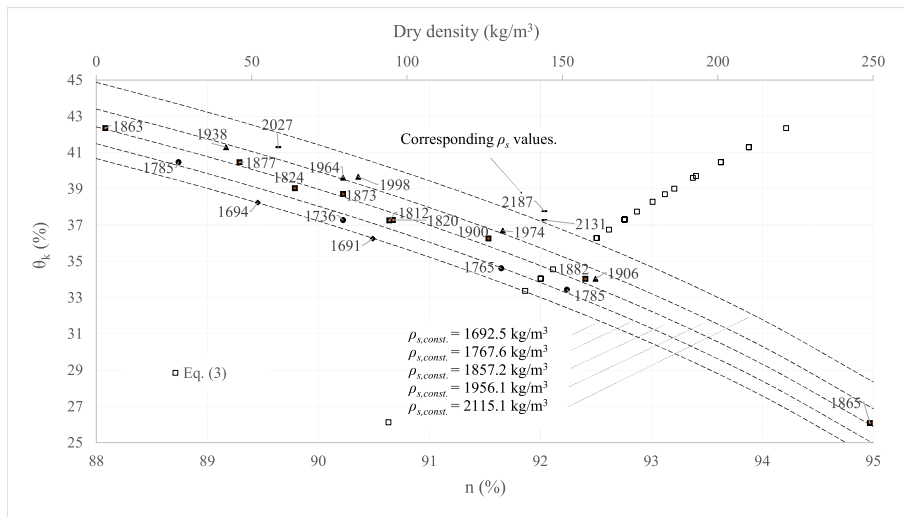


Fig. 4. Influence of landfill settlements on the θ_k values in the early operational stages of a bioreactor landfill.

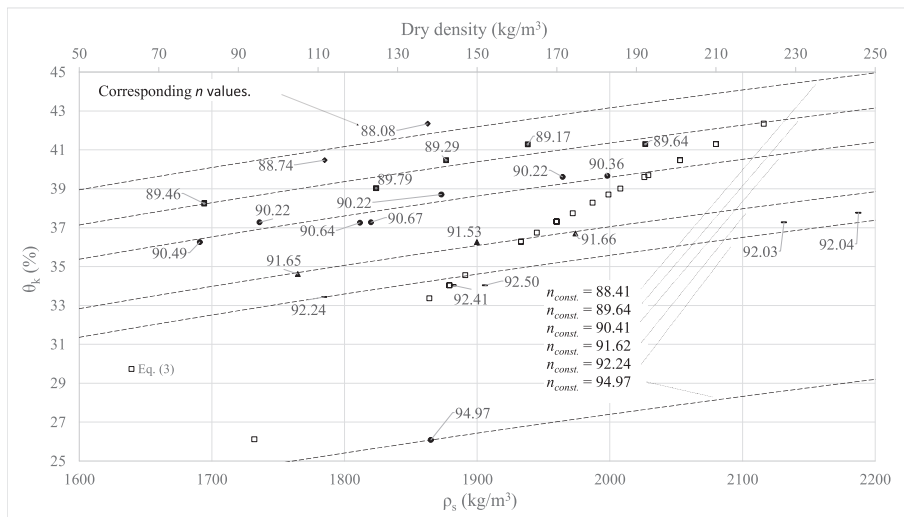


Fig. 5. Influence of degradation process on the θ_k values in the later operational stages of a bioreactor landfill.

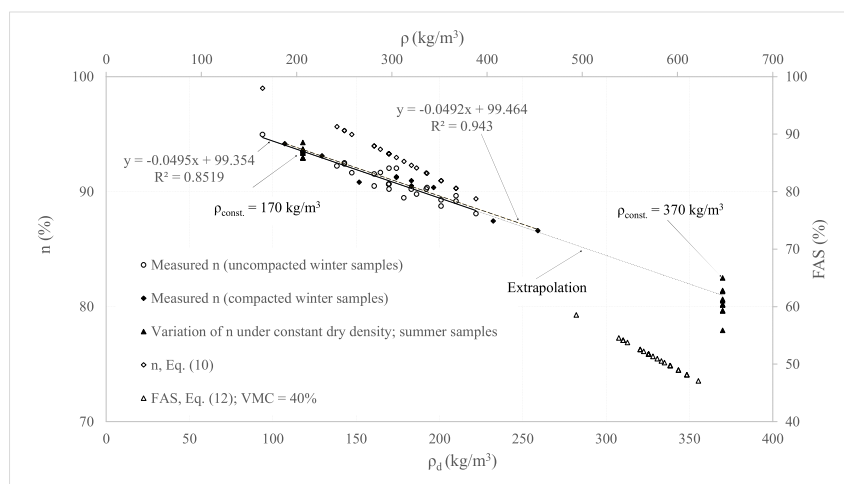


Fig. 6. Relationship between ρ_d and n obtained on winter samples.

probably due to the fact that the MSW samples tested were not pre-treated and, as such, contained a significantly larger amount of closed voids with respect to the MBT waste material used in this research.

The corresponding ρ_d vs. n relationship obtained for compacted waste material (Fig. 6) can be expressed by following Eq. (14):

$$n [\%] = -0.0492\rho_d + 99.464 \quad (14)$$

However, since the variation of measurements lies within the standard deviation of solid particle density of uncompacted samples, for more conclusive evidence of the influence of the compaction process on solid particle density of tested material, further research is necessary.

4.7. Possible application of proposed correlations

For the application of the proposed n vs. θ_k and ρ_s vs. θ_k relationships, it is necessary for a landfill operator to establish the following: a) decrease of waste porosity (n) caused by the wetting procedure; b) degradation stage of the landfilled waste material.

While a decrease in porosity (Δn) can be estimated by various settlement models or by a geodetic survey of the landfill body, the degradation stage can be established through the monitoring of landfill gases. Based on the current degradation stage of an operating landfill, the decrease of ρ_s can be estimated through linear relationships between the degradation stage and ρ_s , which can be found in Reddy et al. (2011) and Yesiller et al. (2014).

Therefore, Eq. (5), along with Eqs. (6) and (7), can be seen as an additional tool for estimating the appropriate field capacity values with respect to the current operational stage of a bioreactor landfill. The proposed equations can be seen as a valuable tool for improving the decomposition process within a landfill body and, consequently, for increasing energy recovery revenues. In addition, a proposed linear ρ_d vs. n correlation can be used to estimate the corresponding dry density of waste material, once the current porosity (n) is known.

For the tested material, Table 4 reveals that the field capacity of landfilled material in the initial stage of the Marišćina landfill should be close to 50%. A further increase in the initial field capacity value, due to settlements caused by the wetting procedure and degradation process in the later operational stages, can be anticipated.

5. Conclusions

It has been demonstrated that θ_k is not only a function of the ρ_d but it is also significantly influenced by more fundamental properties, such as n and ρ_s . Within this research, second degree polynomial n vs. θ_k and first-degree polynomial ρ_s vs. θ_k relationships, applicable to the biodried waste with particle size $D_{50} \approx 5.0$ mm, are derived. A linear ρ_d vs. n correlation is also proposed.

It is important to note that, if the material of interest does not possess similar granulometric properties to the material presented in this manuscript, the use of the proposed relationships is not recommended.

Data availability

All of the data, models, and code generated or used during the study appear in the submitted article.

CRediT authorship contribution statement

Igor Petrović: Conceptualization, Methodology, Validation, Writing, Supervision

Nikola Kaniški: Validation, Investigation

Nikola Hrnčić: Validation, Investigation

Ivan Hip: Validation, Formal analysis, Writing – Review & Editing

Declaration of competing interest

The authors declare the following financial interests/personal relationships which may be considered as potential competing interests: Igor Petrovic reports financial support was provided by Croatian Science Foundation.

Acknowledgements

This work was supported, in part, by the Croatian Science Foundation under the project UIP-2017-05-5157.

Appendix A. Supplementary data

Supplementary data to this article can be found online at <https://doi.org/10.1016/j.biteb.2022.100996>.

References

- ABNT(b), 1984. Grãos de solos que passam na peneira de 4.8 Mm – Determinação da massa específica. (NBR 06508/1984). Associação Brasileira de Normas Técnicas, São Paulo.
- Agnew, J.M., Leonard, J.J., 2002. Using a modified pycnometer to determine free air space and bulk density of compost mixture while simulating compressive loading. In: Michel, F.C., Rynk, R.F., Hoiting, H.A.J. (Eds.), Proceedings of the International Symposium Composting and Compost Utilization, Columbus, OH, USA, pp. 183–204.
- Agnew, J.M., Leonard, J.J., Feddes, J., Feng, Y., 2003. A modified air pycnometer for compost volume and density determination. Can. Biosyst. Eng. 45, 27–34.
- ASTM International, 2007. Standard Test Method for Particle-size Analysis of Soils (Withdrawn 2016) (D422–63). ASTM International, West Conshohocken, PA.
- ASTM International, 2016a. Standard Test Methods for Specific Gravity of Soil Solids by Water Pycnometer (D854–14). ASTM International, West Conshohocken, PA.
- ASTM International, 2016b. Standard Test Methods for Maximum Index Density And Unit Weight of Soils Using a Vibratory Table (D4253–16e1). ASTM International, West Conshohocken, PA.
- ASTM International, 2019. Standard Test Methods for Laboratory Determination of Water (Moisture) Content of Soil And Rock by Mass (D2216–19). ASTM International, West Conshohocken, PA.
- ASTM International, 2020. Standard Test Methods for Determining the Water (Moisture) Content, Ash Content, And Organic Material of Peat And Other Organic Soils (D2974–20e1). ASTM International, West Conshohocken, PA.
- Beaven, P.R., 1999. The Hydrogeological And Geotechnical Properties of Household Waste in Relation to Sustainable Landfilling. University of London. PhD diss.
- Blight, G.E., Ball, J.M., Blight, J.J., 1992. Moisture and suction in sanitary landfill in semiarid areas. J. Environ. Eng. 118 (6), 865–877.
- Breitmeyer, R.J., 2011. Hydraulic Characterization of Municipal Solid Waste. University of Wisconsin-Madison. PhD diss.
- Breitmeyer, R.J., Benson, C.H., 2011. Measurement of unsaturated hydraulic properties of municipal solid waste. In: Geo-frontiers 2011: Advances in geotechnical engineering, ASCE, pp. 1433–1442.
- British Standards Institution, 1990. Methods of Test for Soils for Civil Engineering Purposes - Classification Tests (BS 1377-2:1990), London, United Kingdom.
- Buivid, M.G., Wise, D.L., Blanchet, M.J., Remedios, E.C., Jenkins, B.M., Boyd, W.F., Pacey, J.G., 1981. Fuel gas enhancement by controlled landfilling of municipal solid waste. Resour. Conserv. 6, 3–20.
- Christensen, T.H., Cossu, R., Stegman, R. (Eds.), 1989. Sanitary Landfilling: Process, Technology And Environmental Impact, first ed. Elsevier, Amsterdam.
- Cossu, R., Stegman, R., 2019. Solid Waste Landfilling – Concepts, Processes, Technology, first ed. Elsevier, Amsterdam.
- Entenmann, W., Wendt, P., 2007. Placement and compaction of treated municipal solid waste in modern landfills, results of geotechnical and hydraulic tests and monitoring. In: Proc. of the Sardinia 2007, Eleventh International Waste Management and Landfill Symposium, Cagliari, Italy.
- Fungaroli, A.A., 1971. Pollution of Subsurface Water by Sanitary Landfills. Interim Report, Vol. I. Environmental Protection Agency, United States <https://babel.hathitrust.org/cgi/pt?id=mdp.39015095042274&view=1up&seq=4&skin=2021/> (accessed 15 November 2021).
- Fungaroli, A.A., Steiner, R.L., 1979. In: Vol. I. (Ed.), Investigation of Sanitary Landfill Behavior. Final Report. Drexel University, Philadelphia, Pennsylvania.
- Gabr, A., Valero, S.N., 1995. Geotechnical properties of municipal solid waste. Geotech. Test. J. 18 (2), 241–251.
- Gao, W., Chen, Y., Zhan, L., Bian, X., 2015. Engineering properties for high kitchen waste content municipal solid waste. J. Rock Mech. Geotech. Eng. 7, 646–658.
- Hudson, A.P., White, J.K., Beaven, R.P., Powrie, W., 2004. Modelling the compression behaviour of landfilled domestic waste. Waste Manag. 24, 259–269.
- Hyun Il, P., Borinara, P., Hong, K.D., 2011. Geotechnical considerations for end-use of old municipal solid waste landfills. Int. J. Environ. Res. 5 (3), 573–584.
- Ke, H., Jie, H., Xu, X.B., Wang, W.F., Chen, Y.M., Zhan, L.T., 2017. Evolution of saturated hydraulic conductivity with compression and degradation for municipal solid waste. Waste Manag. 65, 63–74.

- Lins, E.A.M., Jucá, J.F.T., Lins, C.M.M.S., Mariano, M.O.H., 2020. Relationship of field capacity with geotechnical parameters in an urban solid waste landfill. *ASRJETS* 71 (1), 99–122.
- Mokhtari, M., Heshmati Rafasnjani, A.A., Shariatmadari, N., 2019. The effect of aging on the compressibility behavior and the physical properties of municipal solid wastes: a case study of Kahrizak landfill, Tehran. *Environ. Earth Sci.* 78 (16), 1–14.
- Olivier, F., Gourc, J.-P., 2007. Hydro-mechanical behaviour of municipal solid waste subject to leachate recirculation in a large-scale compression reactor cell. *Waste Manag.* 27, 44–58.
- Pulat, H.F., Yukselen-Aksoy, Y., 2017. Factors affecting the shear strength behaviour of municipal solid wastes. *Waste Manag.* 69, 215–224.
- Ramaiah, B.J., Ramana, G.V., 2017. Study of stress–strain and volume change behavior of emplaced municipal solid waste using large-scale triaxial testing. *Waste Manag.* 63, 366–379.
- Reddy, K.R., Hettiarachchi, H., Parakalla, N.S., Gangathulasi, J., Bogner, J.E., 2009. Geotechnical properties of fresh municipal solid waste at Orchard Hills Landfill, USA. *Waste Manag.* 29 (2), 952–959.
- Reddy, K.R., Hettiarachchi, H., Gangathulasi, J., Bogner, J.E., 2011. Geotechnical properties of municipal solid waste at different phases of biodegradation. *Waste Manag.* 31, 2275–2286.
- Reinhart, D.R., Townsend, T.G., 1998. *Landfill Bioreactor Design And Operation*, first ed. CRC Press, Boca Raton.
- Rose, J.L., Izzo, R.L.S., Mahler, C.F., 2009. Effect of MSW compost-soil mixtures in compaction and permeability tests. In: *Proc. of the Sardinia 2009, Twelfth International Waste Management and Landfill Symposium*, Cagliari, Italy.
- Ruggieri, L., Gea, T., Artola, A., Sanchez, A., 2009. Air filled porosity measurements by air pycnometry in the composting process: a review and a correlation analysis. *Bioresour. Technol.* 100, 2655–2666.
- Sivakumar Babu, G.L., Lakshmikanthan, P., Santhosh, L.G., 2015. Shear strength characteristics of mechanically biologically treated municipal solid waste (MBT-MSW) from Bangalore. *Waste Manag.* 39, 63–70.
- Stoltz, G., Gourc, J.-P., Oxarango, L., 2010. Characterization of the physico-mechanical properties of MSW. *Waste Manag.* 30, 1439–1449.
- Stolz, G., Tinet, A.-J., Staub, M.J., Oxarango, L., Gourc, J.-P., 2012. Moisture retention properties of municipal solid waste in relation to compression. *J. Geotech. Geoenviron.* 138, 535–543.
- Sudarshana, C.K.F., 2011. *Strength Characteristics of Mechanically Biologically Treated (MBT) Waste*. University of Southampton. PhD diss.
- Tchobanglous, G., Theisen, H., Vigil, S.A., 1993. *Integrated Solid Waste Management – Engineering Principles And Management Issues*, first ed. McGraw-Hill, New York.
- Thakur, D., Gupta, A., Ganguly, R., 2019. Geotechnical properties of fresh and degraded MSW in the foothill of Shivalik Range Una, Himachal Pradesh. *Int. J. Recent Technol.* 8, 363–374.
- Velásquez, Ma.T.O., Cruz-Rivera, R., Rojas-Valencia, N., Monje-Ramírez, I., 2003. Determination of field capacity of municipal solid waste with surcharge simulation. *Waste Manag. Res.* 2, 137–144.
- Velis, C.A., Longhurst, P.J., Drew, G.H., Smith, R., Pollard, S.J.T., 2009. Biodrying for mechanical-biological treatment of wastes: a review of process science and engineering. *Bioresour. Technol.* 100, 2747–2761.
- Velkushanova, K., 2011. *Characterization of Wastes Towards Sustainable Landfilling by Some Physical And Mechanical Properties With an Emphasis on Solid Particles Compressibility*. University of Southampton. PhD diss.
- Wei, H.Y., 2007. *Experimental And Numerical Study on Gas Migration in Landfill of Municipal Solid Waste*. PhD diss. Zhejiang University (in Chinese).
- Wu, H., Wang, H., Zhao, Y., Chen, T., Lu, W., 2012. Evolution of unsaturated hydraulic properties of municipal solid waste with landfill depth and age. *Waste Manag.* 32 (3), 463–470.
- Yesiller, N., Hanson, J.L., Cox, J.T., Noce, D.E., 2014. Determination of specific gravity of municipal solid waste. *Waste Manag.* 34 (5), 848–858.
- Geotechnical characterization, field measurement, and laboratory testing of municipal solid waste. In: Zekkos, D. (Ed.), 2008. *Proc. of the International Symposium on Waste Mechanics*, New Orleans, Louisiana, United States.
- Zhan, L.T., Ling, D., Zhang, W.J., Chen, Y., 2008. Hydrogeological characterization of Suzhou landfill of municipal solid wastes. In: *Proceedings of GeoCongress 2008, Geotechnics of Waste Management and Remediation*, ASCE, pp. 248–255.
- Zhu, X., Jin, J., Fang, P., 2003. Geotechnical behavior of the MSW in Tianziling landfill. *J. Zhejiang Univ. Sci.* 4 (3), 324–330.
- Zornberg, J.G., Jernigan, B.L., Sanglerat, T.R., Cooley, B.H., 1999. Retention of free liquids in landfills undergoing vertical expansion. *J. Geotech. Geoenviron.* 125, 583–594.